Lossless 1×2 Optical Switch Monolithically Integrated on a Passive Active Resonant Coupler (PARC) Platform

S. S. Saini, Y. Hu, F. G. Johnson, D. R. Stone, H. Shen, W. Zhou, J. Pamulapati, M. N. Ott, H. C. Shaw, and M. Dagenais, *Senior Member, IEEE*

***Abstract*—In this letter, we demonstrate a lossless 1×2 optical switch utilizing resonant vertical coupling between an active and a passive waveguide. Optical power is coupled into the passive waveguide and split into two ports using a 3-dB Y-junction splitter. The mode is then coupled up to a 1-mm-long active waveguide where gain is provided. A 100-μm-long taper is utilized in each arm for coupling the mode from the passive to the active waveguide. Internal gain greater than 22 dB is obtained in each arm of the integrated splitter. High yield and good uniformity of devices are obtained over multiple processing runs.**

***Index Terms*—Lossless splitters, monolithic integration, optical switch, photonic integrated circuits, resonant couplers, semiconductor optical amplifiers, splitters, twin waveguides.**

I. Introduction

WITH THE increasing complexity of optical modules, there is a need for integrating various active and passive devices on a single substrate to increase the functionality of optical chips. Several approaches for integrating various active and passive devices have been reported [1]–[4]. One of the methods is to use regrowth for creating a low-loss passive waveguide butt-coupled to the active waveguide [1]. Besides being a complex technology, issues like low-loss coupling over multiple runs are still a challenge. A second technique used for integration is selective area growth [2]. The selective area growth technology, in general, does not allow for freedom in the design of the various layer thicknesses and bandgaps of the integrated waveguides. Quantum-well (QW) interdiffusion [3], [4] has also been used for integration by altering the bandgaps of the waveguides but also suffers from a lack of freedom in the design of the waveguide vertical dimensions and in the selection of the proper bandgaps.

Recently [5], [6], we have demonstrated a platform technology called a passive active resonant coupler (PARC) for monolithically integrating active and passive devices in a single epitaxial growth. The PARC platform uses resonant coupling over a taper [6] to couple an optical mode from a highly confined QW region to a well-confined passive waveguide. The active waveguide (AW) consists of four QW's in a separate-confinement heterostructure and is designed to give high gain at 1.55 μm. The passive waveguide (PW) is 0.4 μm thick. It consists of a 20-layer stack of InP and lattice-matched quaternary and is designed for efficient passive devices like splitters and directional couplers. The mode is transformed from the AW to the PW and vice versa, using a 100-μm-long taper with less than 0.06 dB of simulated coupling loss. We have achieved a coupling loss of less than 0.15 dB experimentally. The PARC platform offers attractive features like single epitaxial growth and conventional fabrication techniques. Also, the two waveguides in the platform can be designed independently for their dimensions and bandgaps. This allows for greater freedom in the design of photonic integrated circuits. In fact, in our previous work [7], we have also demonstrated an expanded mode laser on PARC by coupling optical power from an AW to a large loosely confined PW.

In this work, we have designed, fabricated, and demonstrated a lossless 1×2 Y-junction optical switch on the PARC platform demonstrating the utility of the platform for integrating both active and passive devices on a single substrate. In this paper, we discuss the design and the results obtained on the lossless optical switch.

II. Device Design

The schematic of the ridge on the PW used for the 1×2 lossless optical switch is shown in Fig. 1. The optical power is coupled into a 2-μm wide waveguide defined on the PW of the PARC. The input waveguide is 300 μm long and feeds into a 300-μm-long mode expansion region. Here the mode is transformed from the initial 2-μm width to a width of 4 μm. Two 1-mm-long, 2-μm-wide sinusoidal bends are used to split the mode and separate it by 25 μm. The radiation loss over this section of the device is less than 0.6 dB. The PW is then tapered from a 2.0-μm width to the width of 4.5 μm over a 100-μm-long taper. This is done to conform to the coupling previously demonstrated in the PARC platform [5]. The mode is then coupled from the PW to the upper AW using the 100-μm-long taper. The details of the taper are shown in Fig. 2. The PW in the taper section is a constant width of 4.5 μm. The AW is tapered from

Manuscript received November 23, 1999; revised March 9, 2000.

S. S. Saini, Y. Hu, and M. Dagenais are with the Department of Electrical and Computer Engineering, University of Maryland, College Park, MD 20742 USA.

F. G. Johnson and D. R. Stone are with the Laboratory for Physical Sciences, College Park, MD 20740 USA.

H. Shen, W. Zhou, and J. Pamulapati are with the Army Research Laboratory, Adelphi, MD.

M. N. Ott is with Sigma Research and Engineering, NASA Goddard Space Flight Center, Code 562, Greenbelt, MD 20771 USA.

H. C. Shaw is with NASA Goddard Space Flight Center, Code 562, Greenbelt, MD 20771 USA.

Publisher Item Identifier S 1041-1135(00)05595-6.

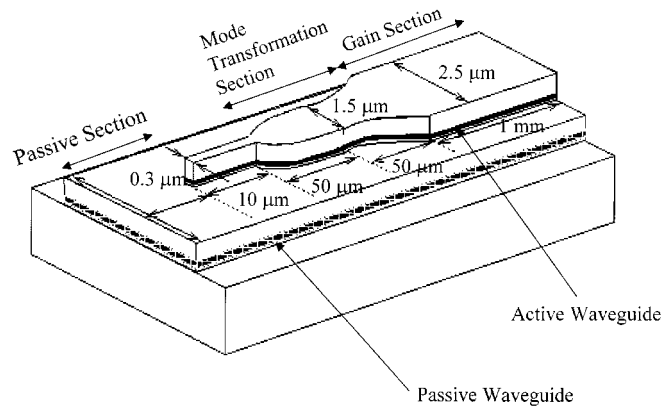

Fig. 1. Schematic of the integrated 3-dB splitter. The ridge on the passive waveguide is shown.

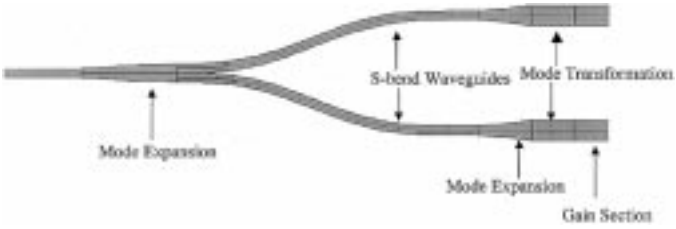

Fig. 2. Schematic of the mode transformation from the passive to the active waveguide. The 1-mm gain sections are also shown.

the initial width of 0.3 μm to a resonant width of 1.5 μm over a 50-μm-long taper of inverse third-order exponential [6]. It is then tapered from the width of 1.5 μm to the final width of 2.5 μm over another 50-μm-long taper using an exponential shape of third order. Previously, this taper shape was shown to have a coupling loss of less than 0.15 dB. A 1-mm-long gain section is incorporated into each arm where the mode is well coupled in the AW.

III. Device Processing

The epitaxial layers were grown using solid source molecular beam epitaxy (MBE) on a 3-in InP substrate. The ridges were defined using a conventional photoresist (OCG-OIR 12 MK) and an optical $10x$-projection aligner. The ridges on the AW were etched to 0.3 μm below the active region. This etch was done using $Ar:Ch_4:H_2$ chemistry in a parallel-plate reactive ion etching (RIE) chamber. No metal or dielectric mask was used for the etching of the sharp tapers. A 4.5-μm-wide, 1-μm-high mesa was then dry etched using the same chemistry to create the confinement for the underlying waveguide and define the 1×2 Y-junction splitter on the PW. A spin-on-glass (SOG) process was used to create the dielectric isolation. This process is self-aligned and eliminates the critical alignment of the dielectric-opening window on top of the ridge. Thus, the whole taper region can be electrically pumped, resulting in a better device performance. The samples were thinned to 100 μm, and p-side (TiPtAu) and n-side (AuNiGeNiAu) ohmic contacts were deposited. The samples were then annealed at 400 °C for 1 min. Using negative photoresist and a metal lift-off process, selective p-side metallization was carried to obtain electrically isolated amplifiers in each arm.

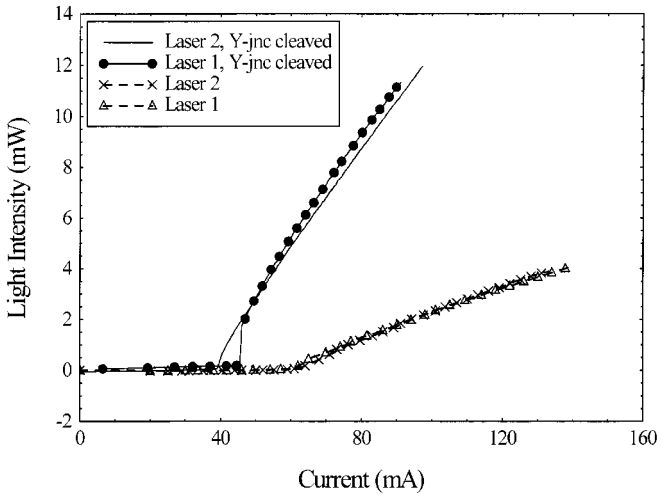

Fig. 3. L–I characteristics for the two amplifiers with and without the Y-junction splitter.

IV. Experiment and Results

The devices were mounted p-side up on copper heat sinks. They were first tested by injecting current into each arm separately and observing the lasing characteristics. The devices lased at a mean threshold current of ∼60 mA and a slope efficiency of ∼0.05 W/A with good uniformity. The Y-junction was cleaved from the gain section for some devices and the L–I curves were again measured. L–I curves for a typical device with and without the Y-junction are shown in Fig. 3. The decrease in threshold and increase in the slope efficiency after cleaving the Y-junction is expected as the reflected power is shared between the two arms in the former device. Comparing these L–I curves, we calculate the excess loss, including the propagation loss in the Y-junction, to be less than 1.5 dB.

The two facets of the device were antireflection (AR) coated ($<10^{-3}$) and the small-signal gain was measured at 1.52 μm by using free space optics to inject an optical signal from a tunable laser source into the PW. As the QW's in the active waveguide are compressively strained, the device will not be polarization-insensitive. Hence, only TE gain was measured. However, the structure can be made to be polarization-insensitive by using tensile strain and will be part of our future direction. Each arm of the splitter was driven separately with 1-μs current pulses and maintained at 20 °C. The coupled input power was determined from a measurement of the sum of the photocurrents across the unbiased arms in the device, with a 100% quantum efficiency assumed. The difference in the photocurrent between the two arms was less than 5%. The measured device internal gain (this does not include the 3-dB split) for both arms is shown in Fig. 4. The difference between the gain in the two arms is less than 1.5 dB. A gain of ∼22 dB was achieved at a current of 275 mA. We have achieved a coupling loss of 1.3 dB to a single-mode fiber from the passive waveguide employed. Assuming this coupling loss to a single-mode fiber at each facet, lossless operation can be obtained at a current of less than 85 mA in this particular device. The on-chip lossless operation is achieved at a current of about 50 mA.

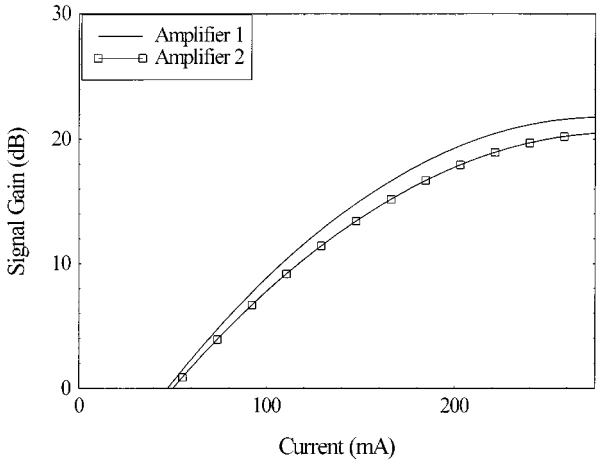

Fig. 4. The internal signal gain in each arm of the splitter. A gain of 22 dB was achieved with less than 1.5-dB imbalance.

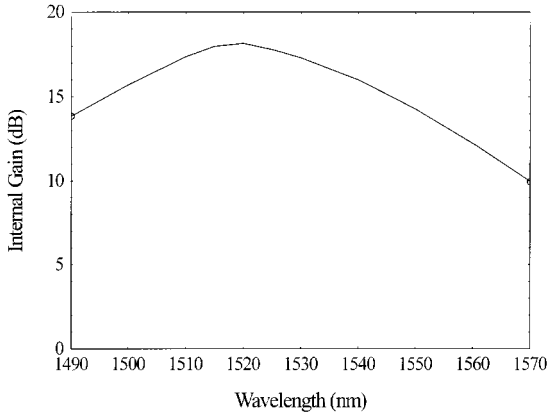

Fig. 5. The internal gain of one arm as a function of wavelength

The measurement of the TE internal signal gain as a function of the input signal wavelength is shown in Fig. 5. A bias current of 200 mA was used for this experiment. The gain is centered at a wavelength of 1520 nm. The gain curve was relatively flat in this region and varies by only 1 dB over a 25-nm range. The saturation output power at a bias of 200 mA was measured to be 10 dBm.

These results are comparable to those reported in the literature for integrated optical switches, which were fabricated using more complex processing and regrowth [8]. As we use single epitaxial growth and conventional fabrication, PARC provides an attractive alternative for monolithic integration of active and passive devices. A yield of greater than 95% was achieved over multiple processing runs. The threshold current variation for various devices without AR coating the facets was less than $\pm 4\%$. Though this data is not exhaustive, it does give indications that high yield can be achieved in the integrated devices based on the PARC platform.

V. Conclusion

We have designed and demonstrated a 1×2 Y-junction optical switch integrated with amplifiers to obtain lossless splitting. On–chip gain of 22 dB after the splitter has been achieved with less than 1.5-dB imbalance between the two arms. The device is designed on our PARC platform and uses resonant coupling over a short taper to couple optical power between an active and a passive waveguide. In this way, we have been able to integrate both active and passive functions on a single platform. This platform uses single epitaxial growth and standard processing techniques. Future work will reduce the length of the Y-junction splitter. A higher ratio lossless splitter is also being designed.

References

[1] J. Wallin, G. Landgren, and K. Streuble, "Selective area regrowth of butt-joint coupled waveguides in multi-section DBR lasers," *J. Cryst. Growth*, vol. 124, no. 1/4, p. 741, Nov. 1992.

[2] J. J. Coleman, R. M. Lammert, and A. M. Jones, "Progress in InGaAs-GaAs selective-area MOCVD toward photonic integrated circuits," *IEEE J. Select. Topics Quantum Electron.*, vol. 3, pp. 874–894, June 1997.

[3] S. Charbonneau, E. S. Koteles, P. S. Poole, J. J. He, G. C. Aers, J. Hayson, M. Buchanan, Y. Feng, A. Delage, F. Yang, M. Davies, R. D. Goldberg, P. G. Piva, and I. V. Mitchell, "Photonic integrated circuits fabricated using ion implantation," *IEEE J. Select. Topics Quantum Electron.*, vol. 4, pp. 772–793, July 1998.

[4] D. Hofstetter, B. Maisenholder, and H. P. Zappe, "Quantum-well intermixing for fabrication of lasers and photonic integrated circuits," *IEEE J. Select. Topics Quantum Electron.*, vol. 4, pp. 794–802, July 1998.

[5] M. Dagenais, S. S. Saini, V. Vusirikala, R. Whaley, F. G. Johnson, and D. Stone, "Alignment tolerant structures for ease of passive packaging," *Proc. SPIE*, vol. 3626, pp. 128–137, 1999.

[6] S. S. Saini, F. G. Johnson, Z. Dilli, Y. Hu, R. Grover, D. R. Stone, H. Shen, J. Pamulapati, W. Zhou, and M. Dagenais, "Compact low-loss vertical resonant mode coupling between two well-confined waveguides," *Electron. Lett.*, vol. 35, no. 14, pp. 1195–1197, July 1999.

[7] S. S. Saini, V. Vusirikala, R. Whaley, F. G. Johnson, D. Stone, and M. Dagenais, "Compact mode expanded lasers using resonant coupling between a 1.55 μm InGaAsP tapered active region and underlying waveguide," *IEEE Photon. Technol. Lett.*, vol. 10, pp. 1232–1234, Sept. 1998.

[8] K. Hamamoto, T. Sasaki, T. Matsumoto, and K. Komatsu, "Insertion loss-free 1×4 optical switch fabricated using bandgap-energy-controlled selective MOVPE," *Electron. Lett.*, vol. 32, no. 24, pp. 2265–2266, Nov. 1996.